Machinery & Energetics
Vol. 13, No. 3. 2022

Journal homepage:
https://technicalscience.com.ua/en

UDC 539.3:539.42:624.012
DOI: 10.31548/machenergy.13(3).2022.34-42

Anastasiia Kutsenko[1*], Oleksii Kutsenko[2]

[1]National University of Life and Environmental Sciences of Ukraine
03041, 15 Heroiv Oborony Str., Kyiv, Ukraine

[2]Taras Shevchenko National University of Kyiv
01033, 60 Volodymyrska Str., Kyiv, Ukraine

Effect of Reinforcement on the Crack Resistance of Concrete Slabs

Abstract. A preliminary analysis of the available publications devoted to the study of crack resistance of reinforced concrete structures showed the absence of established general patterns of influence of important geometric parameters inherent in reinforced concrete elements on the distribution of the characteristics of fracture mechanics along the crack front. Based on the analysis, the purpose of the study was formulated: to establish these regularities for a concrete slab reinforced with a system of longitudinal steel rods. When conducting the research, a linear and elastic model of concrete was used, and the stress intensity factor was considered as a characteristic of the fracture mechanics. A surface crack of constant depth located in the cross-section of the slab was postulated. It was assumed that its faces completely cover the cross-section of reinforcing rods. The crack depth, the depth of reinforcing rods, their diameter, and the distance between adjacent rods were chosen as dimensionless geometric parameters relative to the thickness of the slab. The slab was loaded with two types of loads applied to its ends: constant tensile stresses (pure tension) and linearly variable axial stresses (pure bending). The problem of determining the stress intensity coefficient depending on geometric parameters was reduced to the boundary problem of elasticity theory. The CalculiX finite element analysis package was used to solve it and obtain the stress-strain state of the slab. More than four hundred finite element models were constructed for various combinations of parameters. Based on the known displacements of the crack face points, the values of the stress intensity factor along the crack front were calculated using the relation obtained in the study. It is established that its values significantly depend on the diameter of the reinforcement, and therefore, when conducting practical calculations, it is not recommended to replace the action of reinforcement on concrete with concentrated force. Polynomial approximations with a relative error of 10% are obtained for extreme values of the stress intensity factor. The materials of the study can be useful in the design of reinforced concrete structures, and when studying or teaching a course in fracture mechanics

Keywords: fracture mechanics, stress intensity factor, reinforced concrete structures, finite element method, CalculiX package

Article's History: Received: 05/18/2022; Revised: 06/29/2022; Accepted: 07/18/2022

INTRODUCTION

Issues of crack resistance of reinforced concrete structures (RCS) have been relevant for almost as long as the RCSs themselves exist, that is, for more than a century and a half. Such an insatiable interest in this topic is explained by its direct attitude to ensuring the safe operation of residential, public, and industrial constructions, because almost every modern construction includes reinforced concrete elements. Disregard for the rules and regulations of operation of such facilities is unacceptable and can lead to serious consequences. In this context, it is enough to recall only the case of the "worn-out" Shuliavsky bridge in Kyiv [1], when, under a favourable set of circumstances, there were no human casualties.

Historically, most of the publications devoted to the crack resistance of RCSs are experimental in nature. This circumstance is explained by the relative simplicity of manufacturing experimental samples and the guaranteed reliability of the results of field experiments. Theoretical studies of the crack resistance of RCSs for a long time remained at

Suggested Citation:
Kutsenko, A., & Kutsenko, O. (2022). Effect of reinforcement on the crack resistance of concrete slabs. *Machinery & Energetics,* 13(3), 34-42.

*Corresponding author

the level of model representations and were of little use for direct practical application. The situation began to change in the last two decades, when the development of – programme codes, primarily finite element analysis software, and computer technology allowed modelling the complex structure of RCSs with sufficient discreteness, capable of reproducing an adequate picture of the stress-strain state (SSS) of the reinforced concrete elements under study.

It is worth noting that concrete is generally a physically nonlinear material [2]. Therefore, many concepts of nonlinear fracture mechanics have emerged and/or found their further development in the study on crack resistance of concrete structures. Among them, it is worth noting the two-parameter criterion of local destruction, which in Ukrainian literature is usually referred to as the Leonov-Panasyuk-Dugdale model [3]. Other concepts used in the study of crack resistance of concrete elements include: the pre-destruction zone, the law of sample thickness, the fracture resistance curve (R-curve), etc. A fairly complete overview of the corresponding models is given in [4].

Despite the physical nonlinearity of concrete, the results of many studies [5-7] indicate the possibility of using linear fracture mechanics (LFM) methods to assess the state of cracks in concrete structures. One of the circumstances that facilitate this is the relatively large size of these structures, and the condition for the legality of using LFM is the small plastic zone in the vicinity of the crack vertex compared to the crack length [8]. The length of the macro-crack by definition should be commensurate with the characteristic size of the body in which it is located (otherwise, it refers to micro-cracks, the growth patterns of which are studied by methods of fatigue theory). Consequently, with given mechanical properties of the material, an increase in the size of the body increases the legality of using LFM in the study of its crack resistance. Based on the above, it can be argued that determining the characteristics of LFM in RCSs is of theoretical and practical interest. A significant amount of work is devoted to the investigation of the effect of reinforcement on the distribution of the values of the stress intensity factor (SIF), which is the main characteristic of LFM, along the crack front. The study will briefly consider papers that have a similar object of research.

The study [9] considered a reinforced concrete rod having an edge crack of constant depth located in some of its cross-section. Under assumption that the rod is in a deformable state of bending two approaches to determining the SIF of such a crack, are proposed: analytical and based on finite element modelling. According to the analytical approach, the stress state in the cross-section of the crack location was approached as the stress state of the rod, the cross-section height of which is less than the cross-section height of the original rod by the crack length. The nonlinear relationship between stresses and deformations inherent in concrete was also considered. From the condition of compatibility of deformations of concrete and reinforcement and Hooke's law, the stresses acting in the reinforcement were determined. In the future, the effect of reinforcement on the stress state of concrete was modelled by a concentrated force equal to the equivalent of the specified stresses, that is, their product on the cross-sectional area of reinforcement. The estimated stresses obtained in this way in the vicinity of the crack vertex were considered, in fact, as nominal load stresses in the Griffiths crack problem, and the SIF value itself was established based on the Griffiths formula. The numerical solution, which was based on classical linear fracture mechanics and the finite element method, was implemented using standard tools of the ANSYS software suite. The methods were compared for a single set of geometric and mechanical parameters. The discrepancy in the SIF values obtained by analytical and numerical methods was 1.3% for a certain value of the external bending moment. However, it increased rapidly with a slight increase in bending moment. Thus, with an increase in the moment by one and a half times, the discrepancy increased by an order of magnitude. The authors explain this by the fact that, unlike the numerical value of SIF, the analytical value does not depend linearly on the external moment.

The study [10] also considered a reinforced concrete rod having an edge crack of constant depth located in its cross-section. It is indicated that the simulation was performed using the ANSYS finite element analysis software suite. However, no geometric parameters indicating the relative position of the crack and reinforcement are reflected in the model description. The main conclusion made in the above paper is the significant dependence of the rod stiffness and the stress intensity factor on the rod width. This conclusion was also made on models with slightly variable geometric parameters: only the width of the rod changed within 50%.

In [11] the effect on the crack resistance of a concrete sample of a system of steel reinforcing bars located in it in a plane perpendicular to the external bending moment as a vector was investigated. In this case, some of these rods passed through the faces of a flat edge crack, which was postulated in the cross-section of the sample. As in the above studies, the effect of reinforcement on the stress state of concrete was modelled by concentrated forces. Although the paper provides an expression for SIF for the crack under study, which is based on the assumption of the flat nature of the problem and the superposition principle, the main attention in analysing the results is focused on the dependence of the stiffness of a reinforced concrete sample on the geometric and mechanical properties of its components.

Obviously, this review does not claim to be complete, but it reflects the main trends of such studies: the characteristics of LFM, if calculated, are only for very limited variations in the parameters of the concrete-reinforcement system. This restriction does not provide general conclusions about the criticality of a particular RCSs defect, depending on its size and the parameters of the reinforcement frame. Therefore, the purpose of this study is to determine the stress intensity factor depending on the geometric characteristics of a reinforced concrete element with a crack: the depth of the crack, the thickness of reinforcing rods and the parameters of their location. The originality of the study is

explained by the lack of similar results in available papers, and its relevance is explained by the need to create a handbook of RCS defects that can help quickly assess the danger of defects in practice. The presence of these dependencies also allows analysing the fatigue growth of cracks. A separate goal of the study is to evaluate the validity of modelling the effect of reinforcement on the stress state of concrete with concentrated force, which is often used in theoretical studies, based on numerical results.

MATERIALS AND METHODS

The analysis of the influence of reinforcement on the crack resistance of RCSs will be carried out on the example of a reinforced concrete plates (slabs). Reinforced concrete slabs (RCPs) are one of the most commonly used structural elements in construction. The floor overlaps of most multistorey constructions, the walls of panel houses, the foundations of low-rise buildings – all these components are made in the form of RCPs [12]. As a result, this structural element is very variable in its size, shape, and configuration of reinforcement frames. Therefore, to assess their crack resistance, it is necessary to investigate the patterns of the influence of reinforcement on the distribution of SIF along the front of hypothetical cracks that may occur in RCP.

Problem statement. The study considers a concrete rectangular slab of length L, width W, and thickness h, reinforced with longitudinal steel rods in increments $2s$ by the width of the slab (Fig. 1a). The axes of the reinforcement bars are located at a distance of a from the lower surface of the slab, and their diameter is equal to d. It is assumed that in such a slab, in some of its cross-section, an edge crack of constant depth l has occurred, which is greater than the depth of the reinforcement: $l>a+d/2$. In other words, the face of the crack completely covers the reinforcing rods in the cross-section of its location.

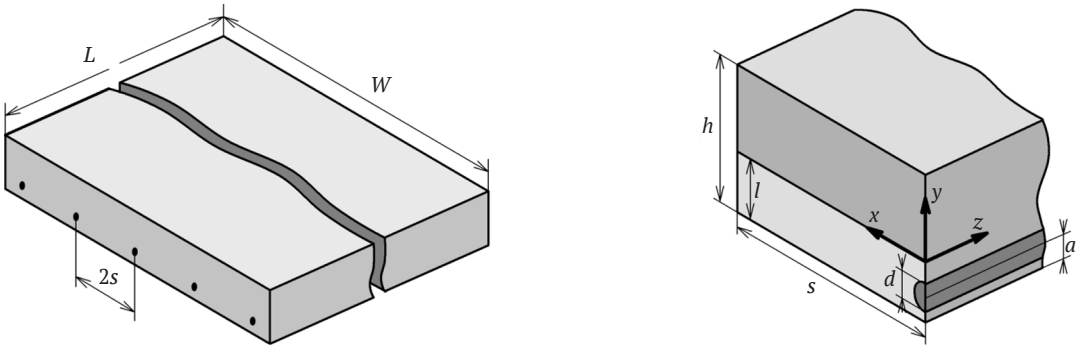

Figure 1. Geometry of the problem: a) general view of RCP; b) half-period of RCP

As an external load, the longitudinal stresses applied to the ends of the slab are considered: constant tensile stresses p (Fig. 2a) and linearly distributed stresses of maximum intensity p (Fig. 2b). The first type of load corresponds to the pure tension of the slab, and therefore, the results associated with it will be denoted by index N. The second type of load determines the pure bend ing of the slab, and therefore, the corresponding results will be denoted by index M. Due to the immutability of the load along the width of the slab, its stress-strain state will have a periodic character along the transverse direction. Therefore, to find it, it is enough to consider only a strip of width s – one half-period of the slab, which is shown in Fig. 1b. A coordinate system associated with a half-period is introduced: its axis x is directed along the crack front, axis y is directed vertically upwards and intersects the axis of the reinforcement rod, and the axis z is directed along the rod, which is shown in Figure 1b in dark grey. In this case, the area of the crack edge shown in Fig. 1b is highlighted in a light gray shade, set by the conditions $z=0$ and $y<0$. It will be also assumed that the plane of the crack location is located at a sufficiently large distance from plate end compared to s. In this case, the influence of edge effects on the stress distribution near the crack front can be ignored and it is assumed that it is symmetric with respect to the plane xy, and therefore, it is enough to consider the SSS of only one half of the slab period, for example, $z>0$.

Figure 2. Plate load: a) σ_{zN} (tension); a) σ_{zM} (bending)

Thus, the following problem is obtained: it is necessary to find the stress-strain state of an elastic body in the form of a rectangular parallelepiped, shown in Fig. 1b, if its surface is free of tangential stresses, and: the side surfaces $y=-l$ and $y=h-l$ and the surface of the crack face ($z=0$ and $y\leq 0$ except for the cross-section of the reinforcement) are also free from normal stresses, on the rest of the end face $z=0$ ($y>0$ without the cross-section of the reinforcement) are free of normal stresses; rest of end $z=0$ and two sides $x=0$ and $x=s$ because of symmetry conditions are of normal

displacements; and at the far end $z=D$ ($D \gg h$) normal stresses are prescribed as:

$$\sigma_{zN}=p=const \quad \text{or} \quad \sigma_{zM}=2p(h/2-l-y)/h. \tag{1}$$

The problem statement is completed by setting the elastic properties of the material. Elastic modulus E and the Poisson's ratio v of concrete will be considered equal to 24 GPa and 0.2, respectively, which corresponds to the design values of concrete class C20/25 [13].

Note that, according to the statement, the problem contains 4 dimensionless geometric parameters. The following are selected as independent ones:

$$\bar{s}=s/h, \bar{l}=l/h, \bar{a}=a/h, \bar{d}=d/h. \tag{2}$$

As a method for solving this problem, the study will use the finite element method (FEM) implemented in the CalculiX packege. This packege determines SSS in solid deformable bodies of various rheological nature under the action of force and temperature loads [14]. Despite the fact that CalculiX is a free-access software suite, its capabilities are not much inferior to many similar commercial products, and in some aspects, due to the openness of its code, even surpass them. This packege also allows solving problems of fracture mechanics, even in a nonlinear formulation [15]. Fig. 3 shows a general view of the CalculiX finite-element model and its separate part in the vicinity of the reinforcement rod outlet to the crack face at $\bar{s}=1$, $\bar{l}=0.3$, $\bar{a}=0.1$, $\bar{d}=0.1$. The model is formed using 20- and 15-node quadratic elements of type C3D20 and C3D15, respectively.

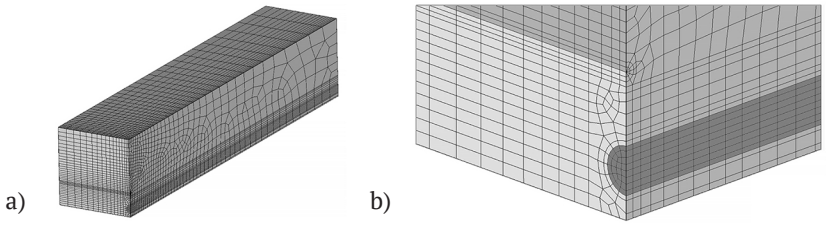

Figure 3. Finite element model for $\bar{s}=1$, $\bar{l}=0.3$, $\bar{a}=0.1$, $\bar{d}=0.1$: a) general view; b) crack face near reinforced rod

Since CalculiX does not have its own SSF estimation tool, it was implemented using additional code. The idea of determining the SIF from pre-calculated SSS is to approximate the field of normal displacements of the points of the crack edges u with an expression $(A++B\rho)\sqrt{\rho}$, where ρ – distance from the displacement determination point to the crack front. Thus, to determine the constans A and B, it is enough to know the displacements u_1 and u_2 at two points near the crack front located at a distance of ρ_1 and ρ_2, respectively. Indeed, substituting the pair of values (ρ_1, u_1) and (ρ_2, u_2) in the expression $u=(A+B\rho)\sqrt{\rho}$, a system of two linear equations is obtained with respect to constants A and B. The field of normal displacements of the crack edges of a normal fracture in the case of plane deformation (the case of the problem formulated) in accordance with the asymptotics of the Westerhard's solution is given by the relation [8; 16]:

$$u = \frac{4(1-\nu^2)}{E\sqrt{2\pi}} K\sqrt{\rho}, \rho \to 0, \tag{3}$$

where the constant K is the stress intensity factor. Comparing expressions $(A+B\rho)\sqrt{\rho}$ and (3), we can conclude that K is proportional to the constant A. Therefore, based on the above relations, the expression for SIF is obtained:

$$K = \frac{E\sqrt{2\pi}}{4(1-\nu^2)} \frac{u_1\sqrt{\rho_2^3} - u_2\sqrt{\rho_1^3}}{\sqrt{\rho_1\rho_2}(\rho_2-\rho_1)}. \tag{4}$$

Equation (4) is the basis for determining the SIF from the known SSS.

To reduce the error in determining the fields in the vicinity of the crack front, it is necessary to move the middle nodes closest to it by a quarter of the length of the corresponding edge of the finite element (FE) towards the corner node lying on the crack front. The specified nodes are circled in Fig. 4a. With this arrangement, the approximations of the stresses fields in the FE near the front will have a root singularity, i.e., they will increase inversely proportional to $\sqrt{\rho}$. Approximations of displacements will decrease to zero proportionally to $\sqrt{\rho}$. This nature of approximations corresponds to the asymptotic solution of the problem of elasticity theory, and therefore, provides greater accuracy of the numerical solution. Similar shift must be made for the middle nodes near the concrete-reinforcement interface line on the crack face (Fig. 4b).

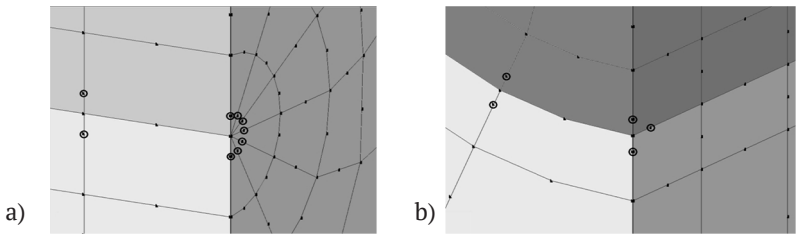

Figure 4. Shift of middle nodes: a) near the front; b) near the interface line on the crack face

Evidently from Figure 3a, a decrease in the dimension of the resolution system was achieved by increasing the FE size in the regions of the period farthest from the crack. The sufficiency of the discreteness of the finite element grid of models was checked by halving the FE size. The relative change in the numerical values of SSF did not exceed 1%.

RESULTS AND DISCUSSION

Using the developed FE models, a large number of calculations of the stresses fields and displacements of the RCP half-period with a crack were performed, based on which the SIF distributions along the crack front were determined. More than 800 SIF distributions were obtained – two for each model (for loads σ_{zN} and σ_{zM}). Figure 5 shows the distribution of normal displacements and normal stresses in the cross-section of the crack edge in the vicinity of the reinforcement rod obtained using the model shown in Fig. 3. The displacements distribution is given for the load case σ_{zN}, and the stresses distribution is for the case of load σ_{zM}. The positive direction of normal displacements is determined by the external normal to the crack face, i.e., in the negative direction of the axis z. The values are given in basic units of the SI system (displacement – in m, stresses – in Pa). The fields are calculated at p=100 MPA and h=0.12 m.

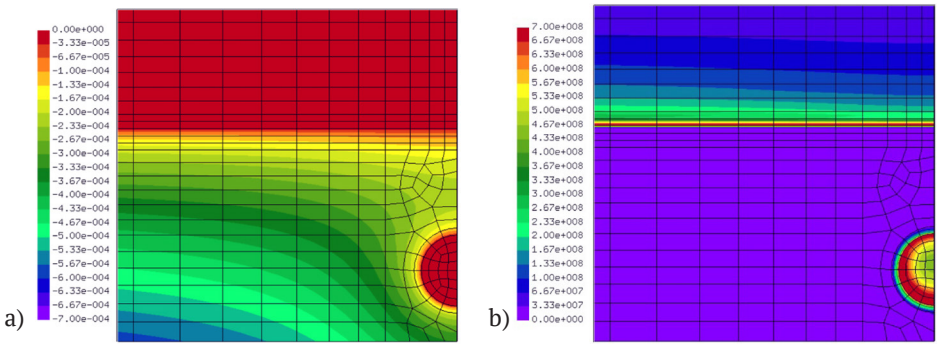

Figure 5. Distribution of fields for $\bar{s}$=1, $\bar{l}$=0.3, $\bar{a}$=$\bar{d}$=0.1:
a) normal displacements field for the load σ_{zN}; b) normal stresses field for the load σ_{zM}

A total of four values of the relative width of the half-period $\bar{s}$: 1, 2, 3, and 5 and three values of the dimensionless diameter of the reinforcement rod $\bar{d}$: 0.05, 0.1, and 0.15 were considered. Dimensionless crack depth $\bar{l}$ varied from 0.05 to 0.7 in increments ranging from 0.25 to 1. The depth of the reinforcement rod $\bar{a}$ axis also varied. At the same time, the obvious conditions for the correctness of the model construction were monitored: a $\bar{a}>\bar{d}/2$ and $\bar{a}+\bar{d}/2<l$. Fig. 6 and 7 show some of the SIF distributions along the front. A dimensionless coordinate is plotted along the abscissa axis of the corresponding graphs $\bar{x}=x/s$, and along the ordinate axis – the value of the dimensionless SIF $\bar{K}=K/(p\sqrt{l})$. The lower index in the SIF designation, as already mentioned, is responsible for the type of load. The numbers in the circles correspond to the parameter $\bar{s}$ values, for which the corresponding distribution was constructed. The value of this parameter for those curves where there are no marks can be determined by analogy. Fig. 6 shows SIF graphs for crack with depth $\bar{l}$=0.3, Fig. 7 – with depth $\bar{l}$=0.7. The dotted lines correspond to the rod diameter $\bar{d}$=0,05, and dashed lines – with a diameter of $\bar{d}$=0.15. The depth of the reinforcement rod axis for all curves was determined by the condition $\bar{a}$=0".025"+$\bar{d}$/2, that is, for all curves, the depth of the reinforcement point closest to the crack front was fixed.

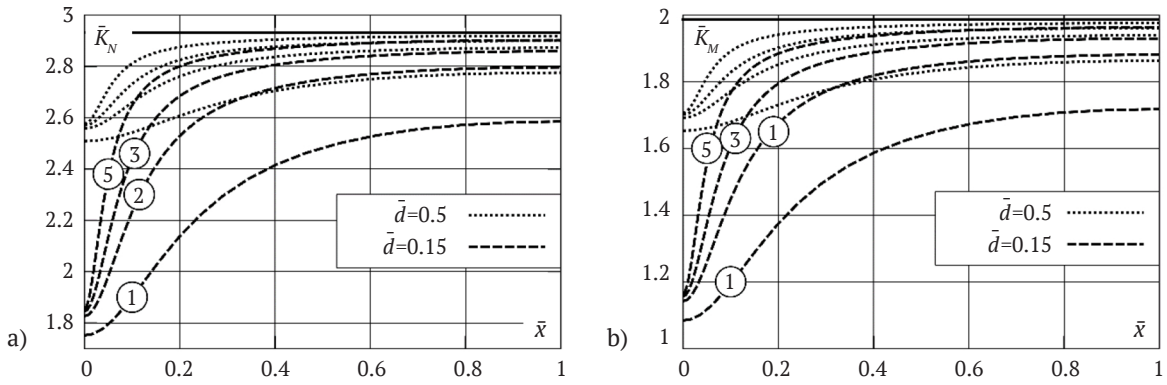

Figure 6. SIF distribution for crack with depth $\bar{l}$=0.3 for loading:
a) σ_{zN}; b) σ_{zM}

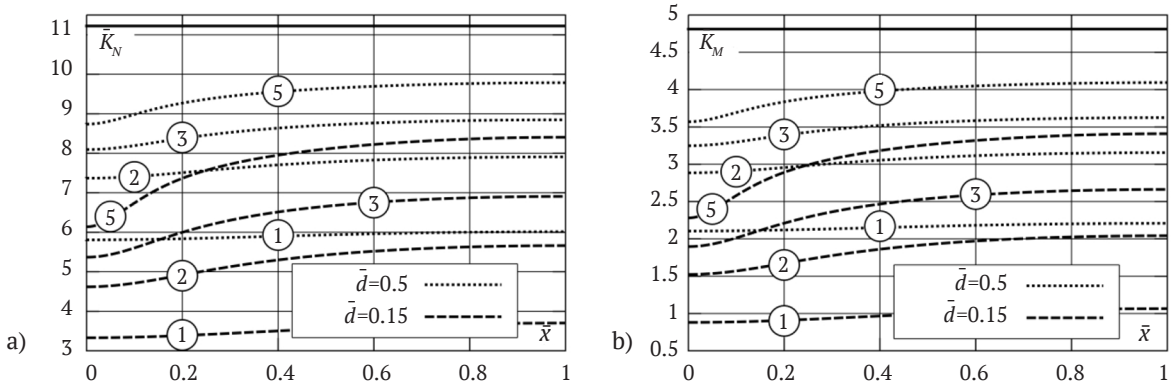

Figure 7. SIF distribution for crack with depth $\bar{l}$=0.7 for loading:
a) σ_{zN}; b) σ_{zM}

In addition to dotted and dashed lines, each of the graphs has a solid horizontal straight line that corresponds to the SIF value in the absence of reinforcement. These values were compared with known in the literature, which are calculated from solutions to the corresponding plane problems. Corresponding exact SIF approximations for tension and bending loads as a function of the only parameter $\bar{l}$ which remains in this case can be represented as [16]:

$$\bar{K}_N = \left(1{,}11 + 5\bar{l}^4\right)\left(1-\bar{l}\right)^{-1}\sqrt{\pi},$$
$$\bar{K}_M = 0{,}7\bar{l}^{-2}\sqrt{\left(1-\bar{l}\right)^{-3} - \left(1-\bar{l}\right)^{3}} \qquad (5)$$

The deviation of the calculated values from (5) does not exceed 1% and 4%, respectively.

Analysing the graphs shown in Figs. 6 and 7, it can be noted that all of them monotonically increase from the minimum value $\bar{K}_{min}=\bar{K}|_{\bar{x}=0}$ near the rod to its maximum value $\bar{K}_{max}=\bar{K}|_{\bar{x}=1}$. The rate of this growth varies. It is largest in the middle part of the front closer to the rod. However, at the neighbourhood of reinforced rod, and at the opposite end of the front, it decreases to zero (the velocity is the derivative, and the derivative is zero at the extreme points). The growth rate in the middle section significantly depends on the diameter of the reinforcement rod: the larger it is, the higher the growth rate, although the values themselves are significantly lower. This conclusion is important in the context of determining the adequacy of replacing the valve action with concentrated force.

Another important conclusion that can be drawn from Figs. 6 and 7, there is a locality of reinforcement action for small cracks. So for a crack with depth $\bar{l}$=0.3, the difference between the maximum and current SIF values is reduced by half at a distance of less than a third of the slab thickness. At the same time, $\bar{K}_{max}$ are much closer to SIF for a flat crack, that is, in the absence of reinforcement. The minimum SIF values, regardless of the crack depth, significantly depend on the reinforcement thickness. In case of a deep crack $\bar{l}$=0.3 they do not depend much on the length of the half-period $\bar{s}$ and already for $\bar{s}\geq 2$ they can be considered constant. For cracks with depth $\bar{l}$=0.7, the minimum SIF values significantly depend on both the rod diameter and the width of the half-period.

Thus, the general conclusion that can be drawn on the basis of the analysis performed is that it is incorrect to replace the arming action with concentrated force during practical calculations. To understand why this is the case, it is necessary to refer to the basic concepts of concentrated force in the mechanics of continuum in general and in elasticity theory in particular. From the course of elasticity theory, it is known [17] that the fields of displacements and stresses in Kelvin, problem, Boussinesq problem and similar three-dimensional problems of elasticity theory have a singularity of the type ρ^{-1} and ρ^{-2}, respectively. Here ρ – distance from the observation point to the point of application of a concentrated force. That is, both take infinite values at the point of application of the concentrated force. According to the solution, looks like the concentrated force "pins out" the point of its application to infinity, which does not correspond to reality. The key to the correct practical use of these singular solutions of elasticity theory lies in the Saint-Venan's principle [17]: replacing the system of external forces with a statically equivalent one has little effect on SSS at remote points. In this case, points located at a distance of at least five characteristic sizes of the area of application of forces are considered remote. In our case, the characteristic size of this area is the diameter of the reinforcement rod. That is, to adequately replace the action of the reinforcement with a concentrated force, it is necessary that the reinforcement rod is at least five of its diameters away from both the crack front and the edge of the slab. Obviously, such conditions cannot be implemented in practice in any way. Therefore, replacing the action of arming with a concentrated force can only be used to explain qualitative behaviour, and not to obtain quantitative results.

For each specific set of parameters (2), a fairly complete picture of the SIF distribution along the crack front can be obtained by knowing two values: $\bar{K}_{min}$ and $\bar{K}_{max}$. Therefore, it is important to be able to find their approximate values using simple relations. To do this, the results obtained were processed using the least squares method. A polynomial approximation of the specified extreme values of SIF as functions of parameters (2)

was found. It turned out that the linear approximation is quite rough and allows a relative error (the ratio of the maximum deviation to the maximum value) of up to 25%. The trade-off between the accuracy and complexity of an expression can be considered an approximation in the form of second-order polynomials. Their relative error for all four values is about 10%. In general, this approximation can be represented as

$$\bar{K}_{ext} = \sum_{i=1}^{4}\sum_{j=i}^{4} \alpha_{ij} r_i r_j + \sum_{i=1}^{4} \beta_i r_i + \gamma, \qquad (6)$$

where *ext* takes one of four values: *Nmin*, *Nmax*, *Mmin*, or *Mmax*; $r_1=\bar{s}$, $r_2=\bar{l}$, $r_3=\bar{a}$, $r_4=\bar{d}$ – indexed geometric parameters (2). The approximation coefficients (6) are shown in Table 1.

Table 1. Approximation coefficients of extreme SIF values

Coefficients	Extreme values of SIF			
	$\bar{K}_{Nmin}$	$\bar{K}_{Nmax}$	$\bar{K}_{Mmin}$	$\bar{K}_{Mmax}$
α_{11}	-8.035×10^{-2}	-1.206×10^{-1}	-4.228×10^{-2}	-6.399×10^{-2}
α_{12}	1.557	2.309	7.727×10^{-1}	1.133
α_{13}	-7.622×10^{-1}	−1.013	-4.148×10^{-1}	-5.643×10^{-1}
α_{14}	9.476×10^{-1}	4.075	5.382×10^{-1}	2.221
α_{22}	9.924	1.680×10	-6.923×10^{-1}	3.291
α_{23}	2.526×10	1.624×10	1.364×10	7.825
α_{24}	-1.100×10^{2}	-1.134×10^{2}	−4.261×10	−5.394×10
α_{33}	−1.107×10	5.066	−4.810	2.301
α_{34}	−5.077×10	3.323×10	−2.014×10	1.933×10
α_{44}	2.548×10^{2}	1.052×10^{2}	1.300×10^{2}	5.129×10
β_1	2.590×10^{-2}	-6.800×10^{-2}	3.867×10^{-2}	1.472×10^{-2}
β_2	−1.868	−8.774	1.299	−2.534
β_3	−5.022	−7.455	−3.386	−3.217
β_4	4.746	1.520×10	−7.413	4.572
γ	2.171	3.873	1.499	2.312

Based on the values in Table 1 and equation (6), it is possible to quickly restore the overall qualitative picture of SIF distributions as a function of geometric parameters. Having distribution data and critical SIF values in concrete, it is possible to quickly give an answer about the degree of danger of a particular defect. In addition, they allow investigating the rate of growth of defects based on the Paris formula [8; 16].

CONCLUSIONS

The problem of crack resistance of RCP was reduced to the problem of linear elasticity theory, which was solved using the CalculiX finite element analysis package for variable values of geometric parameters of the system. In processing the obtained numerical results, general regularities of the dependence of the SIF on the geometric parameters of the RCP are established, namely:

– for all values of geometric parameters, SIF is a periodic and monotonous function on the half-period of the plate width, taking the minimum value near the reinforcing rods, and the maximum value in the middle between them;

– the maximum growth rate of the SIF corresponds to an interval close to its minimum;

– for shallow cracks, the effect of reinforcement is local: the minimum SIF value weakly depends on the length of the slab period, and the SIF itself quickly increases to its maximum value;

– as the rod diameter increases, the difference between the minimum and maximum SIF values increases;

The paper also provides a reasonable warning regarding the modelling of the action of reinforcement on concrete with concentrated force during practical calculations. Instead, it is proposed to use polynomial approximations of extreme SIF values given in the paper and obtained as a result of processing a large array of numerical data to estimate the stress state in the vicinity of the crack front.

Since for real diameters of reinforcing rods, the SIF varies significantly along the front of a flat crack, in order to correctly calculate the crack configuration during its subsidence, this study should be extended to the case of cracks of other configurations, for example, semi-elliptical.

ACKNOWLEDGEMENTS

The authors consider it their duty to express their sincere gratitude to the developers of the CalculiX packege [14] Guido Dhondt and Klaus Wittig for their tremendous and selfless work, the results of which allow researchers around the world to conduct numerical modelling in the field of mechanics free of charge.

REFERENCES

[1] Photo of the day: Shulyavsky bridge collapsed in Kyiv. (2017). Retrieved from https://ukranews.com/ua/news/482055-u-kyyevi-obvalyvsya-shulyavskyy-mist.

[2] Yafei, L., Tao, Z., Jie, Y., Tao, J., Qingfang, Z., & Hexuan, H. (2021). A simplified uniaxial stress-strain curve of concrete and its application in numerical simulation. *E3S Web of Conferences*, 283, article number 01045. doi: 10.1051/e3sconf/202128301045.

[3] Panasyuk, V. (2019). Development of investigations on fracture mechanics of materials and structural integrity: Achievements and perspectives (review). *Procedia Structural Integrity*, 16, 3-10. doi: 10.1016/j.prostr.2019.07.015.

[4] Akram, A. (2021). The overview of fracture mechanics models for concrete. *ACEE*, 14(1), 47-57. doi: 10.21307/acee-2021-005.

[5] Chauhan, D., Tewani, H., & Kalyana Rama, J. (2018). Application of principles of linear elastic fracture mechanics for concrete structures: A numerical study. *Applied Mechanics and Materials*, 877, 282-288. doi: 10.4028/www.scientific.net/AMM.877.282.

[6] Dong, W., Li, J., Zhang, X., & Zhang, B. (2019). Evolutions of SIFs of concrete under sustained loading by considering the effects of stress relaxations. *Journal of Materials in Civil Engineering*, 31(12), article number 04019287. doi: 10.1061/(ASCE)MT.1943-5533.0002949.

[7] Polyakova, I., & Imambayeva, R. (2021). Comparison of the stress-strain state reinforced concrete structures (columns and trusses) with linear and nonlinear statements of the deformation law. *E3S Web of Conferences*, 281, article number 01032. doi: 10.1051/e3sconf/202128101032.

[8] Anderson, T. (2017). *Fracture mechanics: Fundamentals and applications* (4th ed.). London: CRC Press. doi: 10.1201/9781315370293.

[9] Nuguzhinov, Z., Bakirov, Z., Vatin, N., Bakirov, M., Kurokhtina, I., Tokanov, D., & Khabidolda, O. (2021). Stress intensity factor of reinforced concrete beams. *Buildings*, 11(7), article number 287. doi: 10.3390/buildings11070287.

[10] Malipatil, K., & Itti, S. (2019). Stress intensity factor and damage index of reinforced concrete beam. In *Fatigue, durability, and fracture mechanics* (pp. 305-316). Belagavi: Visvesvaraya Technological University. doi: 10.1007/978-981-15-4779-9_19.

[11] Accornero, F., Rubino, A., & Carpinteri, A. (2020). Ductile-to-brittle transition in fibre-reinforced concrete beams: Scale and fibre volume fraction effects. *Material Design & Processing Communications*, 2(6), article number e127. doi: 10.1002/mdp2.127.

[12] Kulikov, P., Ploskyi, V., & Getun, G. (2021). *Constructions of buildings and structures. Book 1*. Kyiv: Lira-K.

[13] DBN V.2.6-98:2009. Constructions of buildings and structures. Concrete and reinforced concrete structures. (2011). Kyiv: Ministry of Regional Construction of Ukraine.

[14] CalculiX: A free software three-dimensional structural finite element program. (2021). Retrieved from http://www.calculix.de.

[15] Bulgakov, V., Aboltins, A., Kutsenko, O., Ivanovs, S., & Pascuzzi, S. (2021). Approximate approach of research and assessment of crack resistance of cylindrical housings. *Engineering for Rural Development*, 20, 1541-1547.

[16] Zrazhevsky, G., Kepich, T., & Kutsenko, O. (2005). *Basics of the theory of strength, deformation and fracture mechanics*. Kyiv: LOGOS.

[17] Sadd, M. (2020). *Elasticity: Theory, applications and numerics* (4th ed.). London: Academic Press.

Анастасія Григорівна Куценко[1], Олексій Григорович Куценко[2]

[1]Національний університет біоресурсів і природокористування України
03041, вул. Героїв Оборони, 15, м. Київ, Україна

[2]Київський національний університет імені Тараса Шевченка
01601, вул. Володимирська, 64/13, м. Київ, Україна

Вплив армування на тріщиностійкість бетонних плит

Анотація. Попередній аналіз наявних літературних джерел, присвячених дослідженню тріщиностійкості залізобетонних конструкцій, показав відсутність встановлених загальних закономірностей впливу важливих геометричних параметрів, властивих залізобетонним елементам, на розподіл характеристик механіки руйнування вздовж фронту тріщини. На основі проведеного аналізу було сформульовано мету дослідження: встановлення зазначених закономірностей для бетонної плити, укріпленої системою поздовжніх арматурних стрижнів. При проведенні досліджень використовувалася лінійно-пружна модель бетону, а у якості характеристики механіки руйнування розглядався коефіцієнт інтенсивності напружень. Постулювалася поверхнева тріщина постійної глибини, розташована в поперечному перерізі плити. Передбачалося, що її береги повність покривають поперечний переріз арматурних стрижнів. У якості безрозмірних геометричних параметрів були обрані віднесені до товщини плити глибина тріщини, глибина залягання арматурних стрижнів, їх діаметр та відстань між сусідніми стрижнями. Плита навантажувалася двома типами навантаження, прикладеними до її торців: постійними розтягуючими напруженнями (чистий розтяг) та лінійно-змінними осьовими напруженнями (чистий згин). Задача визначення коефіцієнта інтенсивності напружень залежно від геометричних параметрів була зведена до граничної задачі теорії пружності. Для її розв'язання і отримання напружено-деформівного стану плити використовувався скінченно-елементний пакет CalculiX. Для різних комбінацій параметрів було побудовано більше чотирьохсот скінченно-елементних моделей. За відомими зміщеннями точок берега тріщини за допомогою співвідношення, отриманого в роботі, розраховувалися значення коефіцієнта інтенсивності напружень вздовж фронту тріщини. Встановлено, що його значення суттєво залежать від діаметра арматури, а тому при проведенні практичних розрахунків дію арматури на бетон не рекомендовано замінювати зосередженою силою. Для екстремальних значень коефіцієнта інтенсивності напружень отримано поліноміальні апроксимації з відносною похибкою в межах 10 %. Матеріали роботи можуть бути корисними при проектуванні залізобетонних конструкцій, а також при вивченні чи викладанні курсу механіки руйнування

Ключові слова: енергоефективність, двигуни середньої потужності, реактивна потужність, внутрішня ємнісна компенсація, компенсувальна ємність, пусковий режим